Three Products Are Better than Two: Entropic Advantages in the Competing Dissociation Reactions of Ionized Azo-*t*-butane

Madlena Rabaev,[†] Anne-Marie Boulanger,[†] David M. P. Holland,[‡] David A. Shaw,[‡] and Paul M. Mayer*,[†]

Chemistry Department, University of Ottawa, Ottawa, Ontario K1N 6N5 Canada, and Daresbury Laboratory, Daresbury, Warrington, Cheshire WA4 4AD, United Kingdom

Received: October 23, 2008; Revised Manuscript Received: December 12, 2008

Ionized azo-*t*-butane (*m/z* 142) undergoes three dissociation reactions: competitive cleavage of the N−C bond to form (1) the *t*-butyl cation ($(CH_3)_3C^+$, *m/z* 57) plus a neutral that is nominally $(CH_3)_3CN_2^\bullet$ (85 Da); (2) *m/z* 85 cation, $(CH_3)_3CN_2^+$, plus the neutral *t*-butyl radical; and (3) a minor rearrangement reaction leading to ionized butene. The competition between channels (1) and (2) is governed by both energetic and entropic considerations as the 85 Da neutral lies in a 1 kJ mol^{-1} potential energy well and when formed dissociates into the *t*-butyl radical and N_2. This gives channel 1 an entropic advantage over channel 2, as long as the transition states for these processes reside close to products, a conclusion supported by threshold photoelectron photoion coincidence spectroscopy, tandem mass spectrometry, and ab initio calculations.

Introduction

When a symmetric molecule or ion can undergo two competing dissociation processes involving the cleavage of the same bond, entropic effects tend to cancel out, and the competition between the two channels is driven primarily by energetic concerns:

$$B{-}A^+ + B^\bullet \leftarrow B{-}A{-}B^{+\bullet} \rightarrow B{-}A^\bullet + B^+ \qquad (1)$$

The mass and thus translational partition functions, $q_{trans}^{\ddagger}$, for the two transition states are the same. The overall geometry of the two transition states should also be similar, producing similar rotational partition functions, $q_{rot}^{\ddagger}$. The only quantity that can vary to any significant extent is $q_{vib}^{\ddagger}$, the vibrational partition functions. Provided the geometric differences between $B{-}A^+$ and $B{-}A^\bullet$ and between $B^\bullet$ and B^+ are not great, the two $q_{vib}^{\ddagger}$ values should also be similar. This is the situation for ionized azo-*t*-butane (*m/z* 142), which undergoes competitive cleavage of the N−C bond to form two sets of products: (1) the *t*-butyl cation ($(CH_3)_3C^+$, *m/z* 57) plus a neutral that is nominally $(CH_3)_3CN_2^\bullet$ (85 Da), or (2) a *m/z* 85 cation, $(CH_3)_3CN_2^+$, plus the neutral *t*-butyl radical (Scheme 1). A third channel, due to a rearrangement reaction, generates ionized butene.

On the surface, the competition between these two channels should be driven by their relative activation energies, E_0, with the respective entropies of activation, $\Delta^{\ddagger}S$, essentially canceling out. The vibrational frequencies for the *t*-butyl neutral and cation are similar, represented by similar ZPE values (both have values of 306.9 kJ mol^{-1} at the B3-LYP/6-31+G(d) level of theory) and $H_0 - H_{298}$ values of 19.89 versus 19.60 kJ mol^{-1}, respectively, and the same could be presumed for the 85 Da neutral and ion (see Results and Discussion). It would be difficult to imagine dramatic differences in the vibrational frequencies and rotational constants of the competing variational transition states for these two channels. To explore this issue further and draw some quantitative conclusions on the above discussion, we have performed threshold photoelectron photoion coincidence spectroscopy and tandem mass spectrometry experiments and ab initio molecular orbital calculations to explore the role of entropy in this competition.

SCHEME 1

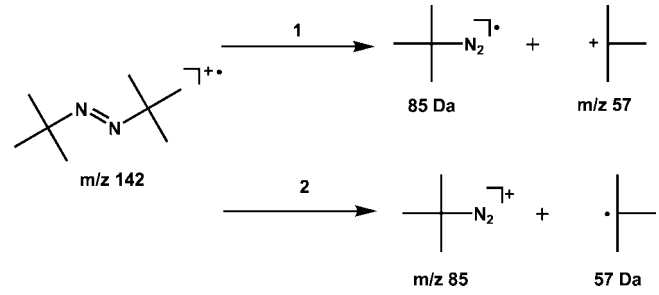

Experimental Procedures

The TPEPICO and TPES experiments were carried out at the Daresbury Laboratory synchrotron radiation source. The TPEPICO spectrometer,[1] the 5 m normal incidence monochromator,[2] and the experimental procedures[3,4] have been described in detail previously. A pulsed extraction technique allowed the breakdown curve to be recorded as a function of precursor ion residence time in the interaction region by changing the time between the detection of the threshold electron and the application of the ion drawout field.[1,4] The minimum residence time in the current apparatus has been measured as 1.116 ± 0.050 μs using the procedure described by Holland et al.[1] The breakdown curve of azo-*t*-butane between photon energies of 7.45 and 8.25 eV has been measured for four ion residence times: 1.116, 3.116, 5.116, and 7.116 μs. The electron transmission function used in the convolution of the calculated breakdown curves was derived from a threshold electron spectrum obtained from the photoionization of krypton in the region of the $^2P_{1/2}$ ionization limit under the conditions used in the TPEPICO measurements.[1]

* Corresponding author. E-mail: pmmayer@uottawa.ca.
[†] University of Ottawa.
[‡] Daresbury Laboratory.

10.1021/jp809404u CCC: $40.75
Published on Web 01/26/2009

The threshold photoelectron spectrum was recorded using only the electron side of the TPEPICO spectrometer[1,5] attached to the 5m normal incidence monochomator.[2] In the spectrometer source region, the monochromatic photon beam interacts with an effusive beam of the gas under investigation, and a small electric field is used to extract threshold (zero kinetic energy) electrons formed through photoionization. The detection system consists of a lens optimized for high transmission of low energy electrons, followed by a hemispherical electrostatic analyzer. After passing through the interaction region, the incident radiation impinges upon a sodium salicylate coated screen, and the resulting fluorescence was detected with a photomultiplier. This signal was used for normalization purposes. The threshold photoelectron spectrum of azo-*t*-butane was measured at a photon resolution of ~10 meV fwhm. The binding energy scale was calibrated by recording a threshold photoelectron spectrum of a gas mixture comprising azo-*t*-butane, xenon, and krypton.

For both the photoelectron photoion coincidence measurements and the threshold photoelectron spectra, a lithium fluoride filter was inserted into the photon beam to suppress higher order radiation.

The mass-analyzed ion kinetic energy (MIKE) and collision-induced dissociation (CID) experiments were performed on a modified VG ZAB mass spectrometer[6] incorporating a magnetic sector followed by two electrostatic sectors (BEE geometry). Ions were generated in the ion source by electron ionization. The pressure inside the ion source was kept at $\sim 1.0 \times 10^{-5}$ Torr as measured with an ionization gauge located above the ion source diffusion pump. Collision-induced dissociation experiments were performed using helium as the target gas. The helium pressure in the collision cell was approximately 8.0×10^{-8} Torr to 1.0×10^{-7} Torr corresponding to a beam reduction of 10%. Collision-induced dissociative ionization (CIDI) experiments[7,8] were carried out by placing He in the first collision cell in the second field free region (2FFR) of the mass spectrometer and O_2 in the second (both with pressures to achieve 10% beam reduction). The deflector electrode between the cells was set at +1000 V to deflect ions out of the beam path.

Materials. Azo-*t*-butane (Aldrich, 97%) was used without further purification for the MIKE and CID experiments. The TPEPICO experiments were performed with azo-*t*-butane (>97%) obtained from Aldrich. The sample was subjected to three freeze−pump−thaw cycles to remove air.

Computational Procedures. Ab initio molecular orbital calculations were performed using the Gaussian 98[9] and 03[10] suite of programs. The azo-*t*-butane neutral, ion, and all fragment ions and neutrals were optimized at the B3-LYP/6-31+G(d) level of theory. This basis set was chosen because it adequately described the geometry and vibrational frequencies of the related 1,1-dimethylhydrazine ion when compared to larger basis sets.[11] A modified G3 protocol[12] based on the optimized B3-LYP/6-31+G(d) geometries and scaled B3-LYP ZPE (scaling factor = 0.9806) was used to calculate the enthalpies of formation of the ions and neutrals.[11,13,14] The optimized structures were used to perform restricted outer valence Green's function (ROVGF) calculations[14] of the molecular orbital ionization energies with the 6-31+G(d) basis set. The molecular orbital coefficients to assign the atomic orbital overlap were obtained using the keyword "pop=full" in Gaussian. The molecular characters were assigned by considering carefully the MO coefficients and MO pictures for each molecular orbital.

A rovibrational RRKM approach[11,13,15] was used to calculate the rate constants ($k(E_{int})$) for the dissociation of the azo-*t*-butane ions. The properties of the transition states were estimated using the parent ion vibrational frequencies and rotational constants. One vibrational mode ($\nu \approx 1000$ cm^{-1}) was removed in the transition state corresponding to the reaction coordinate. The 0 K energy barrier (E_0) and the five lowest vibrational frequencies in the transition state were scaled until a good agreement with the experimental breakdown curves was obtained. To fit the experimental breakdown curves, the RRKM $k(E_{int})$ was convoluted with the electron transmission function, the monochromator bandpass, and the thermal population distribution of the neutral azo-*t*-butane isomer.[11,13] $\Delta^{\ddagger}S_{rovib}$ for the dissociation was calculated in the usual manner[15] employing the scaled transition state vibrational frequencies obtained from the fitting procedure.

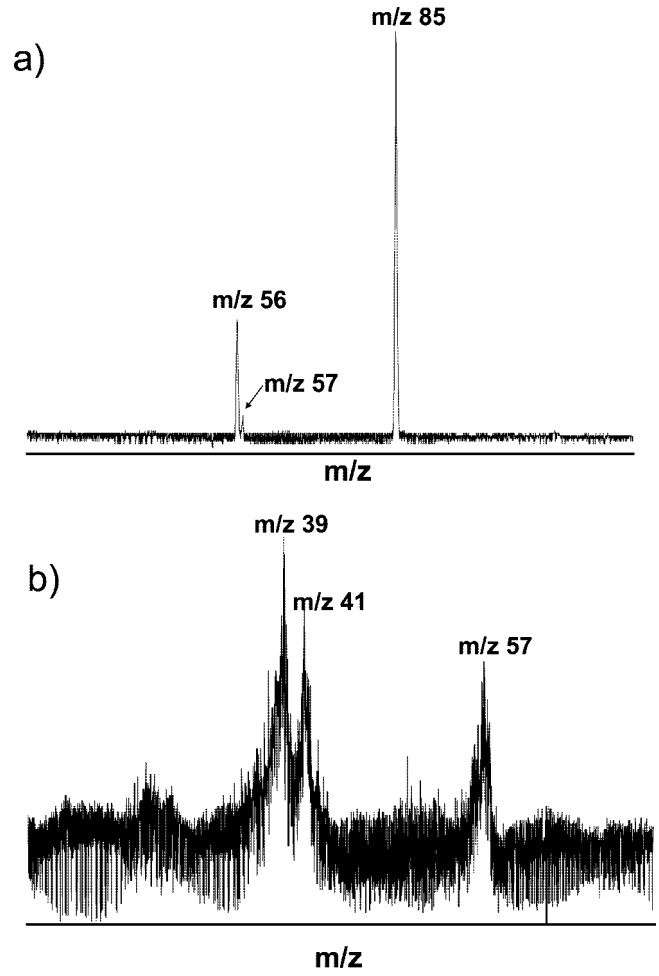

Figure 1. (a) MIKES mass spectrum of *m*/*z* 142 obtained in the 2FFR of the VG ZAB mass spectrometer. (b) CIDI mass spectrum of the collisionally generated neutral with 85 Da.

The tradeoff between energy and entropy when fitting data with RRKM theory can lead to significant uncertainties in the two quantities. The requirement of satisfactory simultaneous fits to four sets of data (corresponding to the four ion source residence times explored in the study) greatly reduces the flexibility in E_0 and $\Delta^{\ddagger}S$. The uncertainties quoted in the Results and Discussion reflect the deviation in these two parameters across all of the acceptable fits.

Results and Discussion

Tandem Mass Spectrometry. The MIKES mass spectrum of metastable *m*/*z* 142 ions is dominated by *m*/*z* 85. Formation of the *t*-butyl cation (*m*/*z* 57) is a minor process, indicating a higher activation energy for this channel. A third, minor, channel

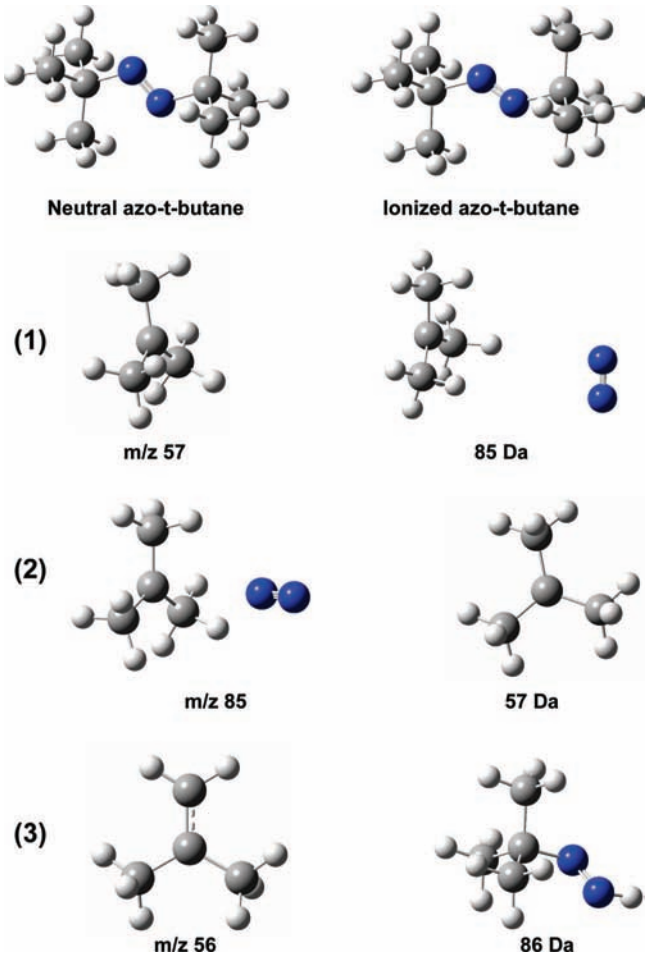

Figure 2. Optimized structures of neutral and ionized azo-*t*-butane and its corresponding fragments from channels (1), (2), and (3).

is present forming ionized butene, *m*/*z* 56 (Figure 1a). Collisional activation results in *m*/*z* 57 becoming the predominant product (relative intensity >90%), indicating a more positive $\Delta^{\ddagger}S$ for this channel than that forming *m*/*z* 85. An attempt was made to characterize the neutral 85 Da $(CH_3)_3CN_2^{\bullet}$ counterpart to the *t*-butyl cation formed in the CID of *m*/*z* 142. A collision-induced dissociative ionization (CIDI) experiment was performed, but the resulting mass spectrum did not contain a *m*/*z* 85 ion, but rather *m*/*z* 57 and its fragmentation products (Figure 1b). This indicates that the neutral moiety with 85 Da either does not survive the 2 μs between the two collision cells in the 2FFR or that it does not survive collisional ionization. The observation of N_2 loss to form *m*/*z* 57 is at least consistent with a neutral that has *t*-butyl and N_2 moieties in its structure. The CID mass spectrum of the metastably generated *m*/*z* 85 ions in Figure 1a was obtained in the 3FFR of the instrument and contained one peak at *m*/*z* 57. Clearly *m*/*z* 85 has a *t*-butyl moiety as part of its structure, suggesting it is $(CH_3)_3CN_2^{+}$. So, tandem mass spectrometry supports the direct bond cleavage reactions proposed in Scheme 1 and suggests that the neutral 85 Da counterpart to the *t*-butyl cation may not be particularly stable on the microsecond time scale.

Ab Initio Calculations. The B3-LYP/6-31+G(d) optimized structures for neutral and ionized azo-*t*-butane and the various fragment ions and neutrals encountered in this work are shown in Figure 2. The G3 energies relative to the azo-*t*-butane molecular ion for the three dissociation channels are 62 kJ mol^{-1} for (1), 52 kJ mol^{-1} for (2), and 259 kJ mol^{-1} for the formation of ionized butene. The latter value clearly indicates that this channel is more complex than the simple H-transfer to form the 86 Da neutral shown in Figure 2. The ion with *m*/*z* 85 optimized to what is in essence an ion−molecule complex between the *t*-butyl cation and N_2 (Figure 2), consistent with the tandem mass spectrometry results, with a binding energy of 12 kJ mol^{-1}. Neutral $(CH_3)_3CN_2^{\bullet}$ is also a complex, a weakly bound van der Waals adduct of N_2 with the *t*-butyl radical. Note that the structure shown in Figure 2 is a transition state structure with one imaginary frequency of −9 cm^{-1}. An equilibrium structure could not be located. The dissociation energy for this species is only 1 kJ mol^{-1}, confirming the suggestion from tandem mass spectrometry that this neutral will immediately dissociate into the *t*-butyl radical plus N_2 once it is formed.

TPEPICO. In TPEPICO spectroscopy, the dominant dissociation channel is (1) forming *m*/*z* 57, while the formation of *m*/*z* 85 and *m*/*z* 56 are minor channels (Figure 3). The time (*t*) window of observation in TPEPICO is $t \leq 1.116$ to $t \leq 7.116$ μs, depending on the ion source residence time, while that for the MIKES experiment is $8 \leq t \leq 15$ μs. The ions generated in the TPEPICO experiment have a distribution of internal energies, starting from $h\nu - IE_a$ (the photon energy less the adiabatic ionization energy) and extending upward according to the thermal energy distribution of the initial neutral molecule. The fact that the TPEPICO observation time window starts at 0 μs after photon absorption means that ions generated with internal energies corresponding to the high energy tail of the internal energy distribution will contribute to the mass spectrum. For these ions, formation of *m*/*z* 57 is the dominant channel. These same high internal energy ions are discriminated against in the MIKES experiment because any ion with a dissociation rate constant greater than 10^6 s^{-1} will dissociate prior to entering the 2FFR of the mass spectrometer.

The breakdown curves at the four delay times (1.116, 3.116, 5.116, and 7.116 μs) are virtually superimposable, indicating that there is no kinetic shift in the fragmentation chemistry. One feature evident from Figure 3 is that the relative contribution of *m*/*z* 85 at low internal energy increases with increasing reaction time, consistent with the fact that it is the dominant channel for low internal energy ions (and thus base peak in the MIKES mass spectrum, Figure 1). The internal energy scale in Figure 3 was determined by subtracting the G3 adiabatic ionization energy (7.40 eV) from the experimental photon energy. The G3 IE is close to that obtained from the onset of the threshold photoelectron spectrum (TPES), 7.55 eV (Figure 4). The TPES reveals a single band at 8.10 eV that corresponds to the vertical ionization of azo-*t*-butane. The ROVGF/6-31+G(d) calculation predicts the highest occupied molecular orbital (HOMO) to be due to the lone pairs on nitrogen and have an energy of 7.978 eV, in good agreement with the experimental result. Both are in excellent agreement with previously reported photoelectron spectra.[16,17]

Six theoretical fits were obtained for the experimental breakdown curves at the four delay times. A representative fit is shown in Figure 3. The reactant ion and transition state vibrational frequencies and rotational constants used in the fitting process are listed in the Supporting Information, Table S1. Note that the poorer fit at the higher internal energies for *m*/*z* 57 and 85 is due to the fact that *m*/*z* 85 itself dissociates to *m*/*z* 57 at these internal energies, as shown by the tandem mass spectrometry and computational results. The average derived E_0 value for formation of *m*/*z* 57 is 0.54 ± 0.01 eV, for *m*/*z* 85 is 0.43 ± 0.01 eV, and for *m*/*z* 56 is approximately 0.41 eV (due to the low intensity of this channel, it was difficult to establish better confidence limits). These compare favorably with the G3

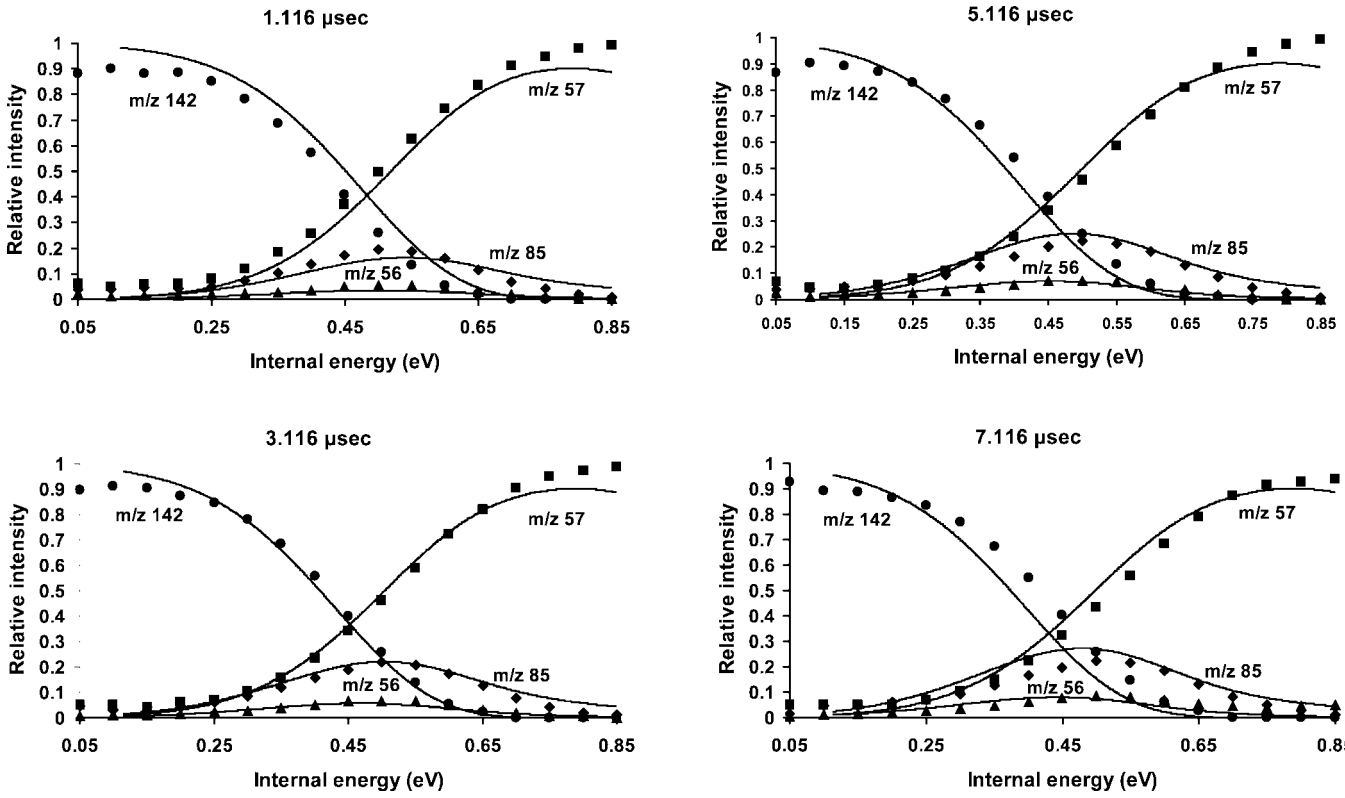

Figure 3. Representative theoretical fit (solid line) to the experimental breakdown curves of *m/z* 142, *m/z* 57, *m/z* 85, and *m/z* 56 at four delay times (1.116, 3.116, 5.116, and 7.116 μs).

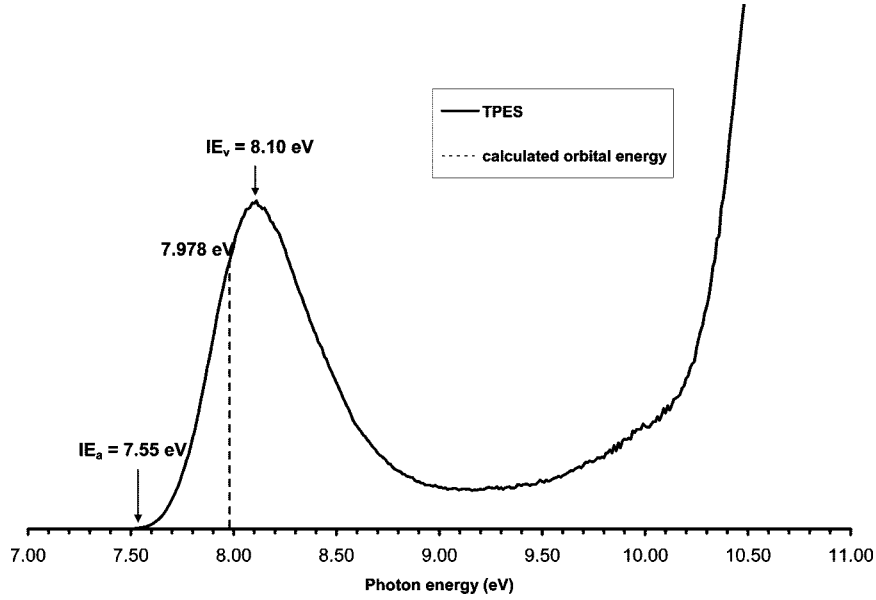

Figure 4. Threshold photoelectron spectrum (TPES) of azo-*t*-butane showing the experimental adiabatic and vertical ionization energies (IE_a and IE_v) and the ROVGF/6-31+G(d) calculated HOMO orbital energy.

threshold values of 0.64 and 0.54 eV for *m/z* 57 and 85, respectively. The products of channel (1) have well-established $\Delta_f H^o$ values and can be used to test the experimental E_0. The sum of the $\Delta_f H^o$ values for the *t*-butyl radical, ion, and N_2 is 759 ± 4 kJ mol^{-1}.[18,19] Subtracting from this the sum of the E_0 value and the G3 IE_a yields a neutral azo-*t*-butane $\Delta_f H^o$ of −7 ± 4 kJ mol^{-1}, in good agreement with the literature value of +1.6 kJ mol^{-1} (obtained by correcting the quoted 298 K value of −36 kJ mol^{-1} to 0 K).[18]

The $\Delta^{\ddagger}S$ values derived for each channel are: 17 ± 1 J K^{-1} mol^{-1} (*m/z* 57), −49 ± 4 J K^{-1} mol^{-1} (*m/z* 85), and −90 J K^{-1} mol^{-1} (*m/z* 56). These values are based on an harmonic oscillator treatment of all vibrational frequencies. If a free rotor model[20] is used for the low frequency torsions, the values become 14 ± 1 J K^{-1} mol^{-1} (*m/z* 57), −44 ± 3 J K^{-1} mol^{-1} (*m/z* 85), and −82 J K^{-1} mol^{-1} (*m/z* 56). In both cases, the entropy of activation for the bond cleavage forming *m/z* 57 is significantly higher than that for the competing cleavage forming *m/z* 85 ($\Delta\Delta^{\ddagger}S$ = ~58 J K^{-1} mol^{-1}). This can be traced to the fact that the neutral counterpart to *m/z* 57 does not exist as a stable species, but rather dissociates to form the *t*-butyl radical and N_2. The formation of three products results in a larger entropy

change in the reaction, which will also mean a larger $\Delta^{\ddagger}S$ if the variational transition state for this process resides close in geometry to the separated products. The difference in the translational entropy change ($\Delta\Delta S_{trans}$) for the two reactions is 145 J K^{-1} mol^{-1}, the difference in the rotational entropy ($\Delta\Delta S_{rot}$) is 45 J K^{-1} mol^{-1} (due almost entirely to the N_2 product), and $\Delta\Delta S_{vib}$ is -81 J K^{-1} mol^{-1}, due primarily to the low frequency vibrations in the *m*/*z* 85 complex that are absent in channel (1) because the 85 Da neutral dissociates. Overall, $\Delta\Delta S$ is 109 J K^{-1} mol^{-1}, and roughly one-half of this is being reflected in $\Delta\Delta^{\ddagger}S$.

Conclusions

Ionized azo-*t*-butane (*m*/*z* 142) undergoes competitive cleavage of the N−C bond to form two sets of products: (1) the *t*-butyl cation ($(CH_3)_3C^+$, *m*/*z* 57) plus a neutral that is nominally $(CH_3)_3CN_2^{\bullet}$ (85 Da), or (2) the *m*/*z* 85 cation, $(CH_3)_3CN_2^+$, plus the neutral *t*-butyl radical. A third, minor, channel leads to ionized butene. Tandem mass spectrometry revealed that the neutral accompanying *m*/*z* 57 may not be stable, but rather dissociates into the *t*-butyl radical and N_2 once formed. This was confirmed by both ab initio calculations of the structure and binding energy of this neutral. The formation of three molecular products in channel 1 means it is characterized by a more positive entropy of activation than is channel 2, as determined by the fitting of TPEPICO spectroscopy breakdown curves using RRKM theory.

Acknowledgment. We are grateful to the Council for the Central Laboratory of the Research Councils (U.K.) for the allocation of beam time at the Daresbury Laboratory Synchrotron Radiation Source. P.M.M. thanks the Natural Sciences and Engineering Research Council of Canada for continuing financial support and the University of Ottawa for seed funds to undertake these experiments.

Supporting Information Available: Table of vibrational frequencies and rotational constants. This material is available free of charge via the Internet at http://pubs.acs.org.

References and Notes

(1) Holland, D. M. P.; Shaw, D. A.; Sumner, I.; Hayes, M. A.; Mackie, R. A.; Wannberg, B.; Shpinkova, L. G.; Rennie, E. E.; Cooper, L.; Johnson, C. A. F.; Parker, J. E. *Nucl. Instrum. Methods Phys. Res., Sect. B* **2001**, *179*, 436.

(2) Holland, D. M. P.; West, J. B.; MacDowell, A. A.; Munro, I. H.; Beckett, A. G. *Nucl. Instrum. Methods Phys. Res., Sect. B* **1989**, *44*, 233.

(3) Rennie, E. E.; Boulanger, A.-M.; Mayer, P. M.; Holland, D. M. P.; Shaw, D. A.; Cooper, L.; Shpinkova, L. G. *J. Phys. Chem. A* **2006**, *110*, 8663.

(4) Rennie, E. E.; Cooper, L.; Johnson, C. A. F.; Parker, J. E.; Mackie, R. A.; Shpinkova, L. G.; Holland, D. M. P.; Shaw, D. A.; Hayes, M. A. *Chem. Phys.* **2001**, *263*, 149.

(5) Boulanger, A.-M.; Rennie, E. E.; Mayer, P. M.; Holland, D. M. P.; Shaw, D. A. *J. Phys. Chem. A* **2006**, *110*, 8563.

(6) Holmes, J. L.; Mayer, P. M. *J. Phys. Chem.* **1995**, *99*, 1366.

(7) Burgers, P. C.; Holmes, J. L.; Mommers, A. A.; Terlouw, J. K. *Chem. Phys. Lett.* **1983**, *102*, 1.

(8) Clair, R.; Holmes, J. L.; Mommers, A. A.; Burgers, P. C. *Org. Mass Spectrom.* **1985**, *20*, 207.

(9) Frisch, M. J.; Trucks, G. W.; Schlegel, H. B.; Scuseria, G. E.; Robb, M. A.; Cheeseman, J. R.; Zakrzewski, V. G.; Montgomery, J. A.; Stratmann, R. E.; Burant, J. C.; Dapprich, S.; Millam, J. M.; Daniels, A. D.; Kudin, K. N.; Strain, M. C.; Farkas, O.; Tomasi, J.; Barone, V.; Cossi, M.; Cammi, R.; Mennucci, B.; Pomelli, C.; Adamo, C.; Clifford, S.; Ochterski, J.; Petersson, G. A.; Ayala, P. Y.; Cui, Q.; Morokuma, K.; Malick, D. K.; Rabuck, A. D.; Raghavachari, K.; Foresman, J. B.; Cioslowski, J.; Ortiz, J. V.; Stefanov, B. B.; Liu, G.; Liashenko, A.; Piskorz, P.; Komaromi, I.; Gomperts, R.; Martin, R. L.; Fox, D. J.; Keith, T.; Al-Laham, M. A.; Peng, C. Y.; Nanayakkara, A.; Gonzalez, C.; Challacombe, M.; Gill, P. M. W.; Johnson, B.; Chen, W.; Wong, M. W.; Andres, J. L.; Gonzalez, C.; Head-Gordon, M.; Replogle, E. S.; Pople, J. A. *Gaussian 98*, revision A.6; Gaussian, Inc.: Pittsburgh, PA, 1998.

(10) Frisch, M. J.; Trucks, G. W.; Schlegel, H. B.; Scuseria, G. E.; Robb, M. A.; Cheeseman, J. R.; Montgomery, J. A., Jr.; Vreven, T.; Kudin, K. N.; Burant, J. C.; Millam, J. M.; Iyengar, S. S.; Tomasi, J.; Barone, V.; Mennucci, B.; Cossi, M.; Scalmani, G.; Rega, N.; Petersson, G. A.; Nakatsuji, H.; Hada, M.; Ehara, M.; Toyota, K.; Fukuda, R.; Hasegawa, J.; Ishida, M.; Nakajima, T.; Honda, Y.; Kitao, O.; Nakai, H.; Klene, M.; Li, X.; Knox, J. E.; Hratchian, H. P.; Cross, J. B.; Bakken, V.; Adamo, C.; Jaramillo, J.; Gomperts, R.; Stratmann, R. E.; Yazyev, O.; Austin, A. J.; Cammi, R.; Pomelli, C.; Ochterski, J. W.; Ayala, P. Y.; Morokuma, K.; Voth, G. A.; Salvador, P.; Dannenberg, J. J.; Zakrzewski, V. G.; Dapprich, S.; Daniels, A. D.; Strain, M. C.; Farkas, O.; Malick, D. K.; Rabuck, A. D.; Raghavachari, K.; Foresman, J. B.; Ortiz, J. V.; Cui, Q.; Baboul, A. G.; Clifford, S.; Cioslowski, J.; Stefanov, B. B.; Liu, G.; Liashenko, A.; Piskorz, P.; Komaromi, I.; Martin, R. L.; Fox, D. J.; Keith, T.; Al-Laham, M. A.; Peng, C. Y.; Nanayakkara, A.; Challacombe, M.; Gill, P. M. W.; Johnson, B.; Chen, W.; Wong, M. W.; Gonzalez, C.; Pople, J. A. *Gaussian 03*, revision C.02; Gaussian, Inc.: Wallingford, CT, 2004.

(11) Boulanger, A.-M.; Rennie, E. E.; Holland, D. M. P.; Shaw, D. A.; Mayer, P. M. *J. Phys. Chem. A* **2007**, *111*, 5388.

(12) Curtiss, L. A.; Raghavachari, K.; Refern, P. C.; Rassolov, V.; Pople, J. A. *J. Chem. Phys.* **1998**, *109*, 7764.

(13) Boulanger, A. M.; Rennie, E. E.; Holland, D. M. P.; Shaw, D. A.; Mayer, P. M. *J. Phys. Chem. A* **2008**, *112*, 866.

(14) Cederbaum, L. S. *J. Phys. B* **1975**, *8*, 290.

(15) Baer, T.; Hase, W. L. *Unimolecular Reaction Dynamics, Theory and Experiments*; Oxford University Press: New York, 1996.

(16) Bock, H.; Wittel, K.; Veith, M.; Wiberg, N. *J. Am. Chem. Soc.* **1976**, *98*, 109.

(17) Houk, K. N.; Chang, Y.-M.; Engel, P. S. *J. Am. Chem. Soc.* **1975**, *97*, 1824.

(18) NIST. *NIST Chemistry Webbook, NIST Standard Reference Database Number 69*; National Institute of Standards and Technology: Gaithersburg, MD, 2000.

(19) Traeger, J. C. *Rapid Commun. Mass Spectrom.* **1996**, *10*, 119.

(20) East, A. L. L.; Radom, L. *J. Chem. Phys.* **1997**, *106*, 6655.

JP809404U